



# Ionic-to-Electronic Conductivity Crossover in CdTe-AgI-As<sub>2</sub>Te<sub>3</sub> Glasses An 110mAg Tracer Diffusion Study

M. Kassem, I. Alekseev, M. Bokova, David Le Coq, E. Bychkov

## ► To cite this version:

M. Kassem, I. Alekseev, M. Bokova, David Le Coq, E. Bychkov. Ionic-to-Electronic Conductivity Crossover in CdTe-AgI-As<sub>2</sub>Te<sub>3</sub> Glasses An 110mAg Tracer Diffusion Study. Journal of Physical Chemistry B, 2018, 122 (14), pp.4179-4186. 10.1021/acs.jpcb.8b00739 . hal-01809150

HAL Id: hal-01809150

<https://univ-rennes.hal.science/hal-01809150>

Submitted on 19 Jun 2018

**HAL** is a multi-disciplinary open access archive for the deposit and dissemination of scientific research documents, whether they are published or not. The documents may come from teaching and research institutions in France or abroad, or from public or private research centers.

L'archive ouverte pluridisciplinaire **HAL**, est destinée au dépôt et à la diffusion de documents scientifiques de niveau recherche, publiés ou non, émanant des établissements d'enseignement et de recherche français ou étrangers, des laboratoires publics ou privés.

1  
2  
3 Ionic-to-Electronic Conductivity Crossover in CdTe-AgI-As<sub>2</sub>Te<sub>3</sub>  
4 Glasses: An <sup>110m</sup>Ag Tracer Diffusion Study  
5  
6

7 M. Kassem,<sup>\*1</sup> I. Alekseev,<sup>2</sup> M. Bokova,<sup>1</sup> D. Le Coq,<sup>3</sup> and E. Bychkov<sup>1</sup>  
8  
9

10  
11 <sup>1</sup>LPCA, Université du Littoral Côte d'Opale ULCO, LPCA, EA CNRS 4493, F-59140 Dunkerque, France  
12  
13

14 <sup>2</sup>V.G. Khlopin Radium Institute, 194021 St. Petersburg, Russia  
15  
16

17 <sup>3</sup>Sciences Chimiques de Rennes, Univ. de Rennes I, 35042 Rennes, France  
18  
19

20 \*E-mail: Mohamad.Kassem@univ-littoral.fr. Phone: +33-328-658270.  
21  
22

23 **ABSTRACT**  
24  
25

26 Conductivity isotherms of (CdTe)<sub>x</sub>(AgI)<sub>0.5-x/2</sub>(As<sub>2</sub>Te<sub>3</sub>)<sub>0.5-x/2</sub> glasses (0.0 ≤ x ≤ 0.15) reveal  
27 a non-monotonic behavior with increasing CdTe content reminiscent of mixed cation  
28 effect in oxide and chalcogenide glasses. Nevertheless, the apparent similarity appears  
29 to be partly incorrect. Using <sup>110m</sup>Ag tracer diffusion measurements, we show that  
30 semiconducting CdTe additions produce a dual effect: (i) decreasing the Ag<sup>+</sup> ion  
31 transport by a factor of ≈200 with a simultaneous increase of the diffusion activation  
32 energy, and (ii) increasing the electronic conductivity by 1.5 orders of magnitude.  
33 Consequently, the conductivity minimum at x = 0.05 reflects an ionic-to-electronic  
34 transport crossover; the silver ion transport number decreases by three orders of  
35 magnitude with increasing x.  
36  
37  
38  
39  
40  
41  
42  
43  
44  
45  
46  
47  
48  
49  
50  
51  
52  
53  
54  
55  
56  
57  
58  
59  
60

## 1           1. INTRODUCTION

2  
3  
4  
5  
6  
7  
8  
9  
10  
11  
12  
13  
14  
15  
16  
17  
Tracer diffusion experiments have been widely used in the past to study ion transport in  
oxide glasses.<sup>1-4</sup> Among the most important results found previously, we should note: (i) the  
diffusion coefficients of alkali cations are significantly higher than those of alkaline-  
earth ions, oxygen species, or glass-forming elements (Si, Al ...); (ii) a diffusivity  
crossover in the mixed alkali glasses; (iii) the Haven ratio  $H_R$  varies systematically,  $0.2 \leq H_R \leq 1$ , depending on the mobile ion content. Nevertheless, until recently, diffusion  
measurements in chalcogenide glasses were rather scarce.<sup>5-7</sup> However, during the last  
decade, several diffusion studies combining both electrical conductivity and radioactive  
tracer diffusion  $D^*$  were presented; thus highlighting phenomena that could not be  
reached by electrical measurements alone.<sup>8-14</sup>

18  
19  
20  
21  
22  
23  
24  
25  
26  
27  
28  
29  
30  
31  
32  
33  
Recently, chalcogenide glasses in the ternary system CdTe-AgI-As<sub>2</sub>Te<sub>3</sub><sup>15</sup> were  
synthesized, and the effect of CdTe semiconductor additives on transport and physical  
properties of binary AgI-As<sub>2</sub>Te<sub>3</sub> glasses has been investigated.<sup>16,17</sup> The glass-forming  
range for (CdTe)<sub>x</sub>(AgI)<sub>0.5-x/2</sub>(As<sub>2</sub>Te<sub>3</sub>)<sub>0.5-x/2</sub> compositions was found to be limited to  $x \leq 0.15$ . The glass transition temperature  $T_g$  decreases in the range  $0.0 \leq x \leq 0.1$  and  
remains constant with further increasing  $x$ . More importantly, the electrical properties  
of cadmium telluride glasses exhibit a non-monotonic behavior with (i) diminished ( $x \leq 0.05$ ) and (ii) enhanced total conductivity  $\sigma_{dc}$  ( $x > 0.05$ ), reminiscent of mixed cation  
effect in oxide and chalcogenide glasses. Semiconducting CdTe additions were assumed  
to produce two distinct phenomena: (i) a decrease of the ionic conductivity by blocking  
the Ag<sup>+</sup> ion transport within the preferential conduction pathways, and (ii) an increase  
of the electronic conductivity caused by Te 5p lone-pair electronic states in the top of  
the valence band.

35  
36  
37  
38  
The present paper deals with <sup>110m</sup>Ag tracer diffusion measurements in the ternary  
(CdTe)<sub>x</sub>(AgI)<sub>0.5-x/2</sub>(As<sub>2</sub>Te<sub>3</sub>)<sub>0.5-x/2</sub> glasses, which would allow to obtain a detailed  
information on the ionic and electronic components of the charge transport.

## 39           2. EXPERIMENTAL DETAILS

### 41           2.1 Glass Preparation

42  
43  
44  
45  
46  
47  
48  
49  
50  
51  
52  
53  
(CdTe)<sub>x</sub>(AgI)<sub>0.5-x/2</sub>(As<sub>2</sub>Te<sub>3</sub>)<sub>0.5-x/2</sub> samples ( $x = 0, 0.01, 0.025, 0.05, 0.075, 0.10, 0.125, 0.15,$   
 $0.17, 0.20$ ) were prepared using the appropriate proportions of CdTe, AgI and As<sub>2</sub>Te<sub>3</sub>.  
The starting materials were sealed under vacuum ( $10^{-6}$  mbar) in a cleaned silica tube (8  
mm ID and 1 mm wall thickness), heated slowly in a rocking furnace to 850 °C at 5 K  
min<sup>-1</sup> heating rate, maintained at this temperature for 24 hours, then cooled down to  
650 °C before quenching in cold salt/water mixture. Several three-gram samples were  
obtained for each composition. Further synthesis details and properties characteristic to  
this telluride system are published elsewhere.<sup>15</sup>

## 2.2 Conductivity Measurements

Total electrical conductivity of the samples was measured using a Hewlett Packard 4194A impedance meter. The impedance modulus  $Z$  and the phase angle  $\theta$  were obtained in the frequency range from 100 Hz to 15 MHz at temperatures between 293 and 378 K, the maximum temperature was below  $T_g$  for the glass samples.<sup>19</sup> The quenched samples, prepared as rectangular plates, were polished using SiC powder (9.3  $\mu$  grain size). The sample sides were ground parallel and gold was deposited on opposite sides to form electrodes for conductivity experiment, i.e., the electrochemical cell for conductivity measurements was Au|glass|Au. Typical thickness and area of the samples were in the range of 0.7-1.5 mm and 6-8 mm<sup>2</sup>, respectively. Further details of conductivity measurements are published previously.<sup>15-18</sup>

## 2.3 <sup>110m</sup>Ag Tracer Experiments

The <sup>110m</sup>Ag tracer (the half-life  $t_{1/2} = 249.76$  d) was produced by the  $^{109}\text{Ag}(n,\gamma)^{110m}\text{Ag}$  nuclear reaction in a research reactor of St. Petersburg Nuclear Physics Institute using thermal neutrons with an average flux of  $8.0(2) \times 10^{13}$  n cm<sup>-2</sup> s<sup>-1</sup>. For each composition, samples having the same conductivity parameters within the experimental uncertainty were used in diffusion experiments. Measurements were carried out using thin-layer geometry. A drop of radioactive <sup>110m</sup>AgNO<sub>3</sub> solution was deposited onto one face of the sample, kept there for 2 h, wiped with a filter paper, washed with distilled water and ethyl alcohol, and then dried. The sample was wrapped in aluminium foil and encapsulated in a Pyrex tube. The samples were annealed in a furnace at 20 to 115 °C for a period of several hours to 60 days. The diffusion anneals were terminated by quenching the samples in air. The sides of the sample parallel to the diffusion direction were ground to eliminate surface diffusion effects. The sample was then sectioned on a parallel grinder. The thickness of each section was determined either from the density, cross-sectional area and weight change of the sample, or by direct thickness measurements. In the latter case, the thickness uncertainty was  $\pm 5$   $\mu\text{m}$ . Further details on tracer diffusion measurements were published elsewhere.<sup>19</sup>

## 3. RESULTS AND DISCUSSION

### 3.1 Tracer Diffusion Results

Penetration profiles for <sup>110m</sup>Ag tracer diffusion in the CdTe-AgI-As<sub>2</sub>Te<sub>3</sub> glasses obey the usual solution of Fick's law for an infinitesimally thin deposit of radioactive isotope on a semi-infinite specimen<sup>2</sup>:

$$1 - \frac{A(y,t)}{A_0} = \operatorname{erf}(q), \quad (1)$$

where

$$q = \frac{y}{2\sqrt{D_{\text{Ag}} t}}, \quad (2)$$

$A(y,t)$  is the residual activity of the sample after a thickness  $y$  was removed,  $t$  is the diffusion anneal time,  $A_0$  is the initial residual activity,  $D_{\text{Ag}}$  is the tracer diffusion coefficient, and  $\text{erf}(q)$  is the Gauss error function. Experimentally determined values of  $A(y,t)$  and  $A_0$  yield  $q$  values which, when plotted vs.  $y$ , produce a straight line passing through the origin, Figure 1.

The silver tracer diffusion coefficients  $D_{\text{Ag}}$ , determined from the slope of the penetration profiles, are given in Figure 2, plotted as  $\log D_{\text{Ag}}$  versus  $T^{-1}$ . Figure 2 shows that the temperature dependences of the tracer diffusion coefficient are in good agreement with Arrhenius-type activation dependence

$$D = D_0 \exp\left(-\frac{E_d}{kT}\right), \quad (3)$$

where  $D_0$  is the diffusion pre-exponential factor,  $E_d$  the diffusion activation energy,  $k$  and  $T$  have their usual meaning. The derived diffusion parameters  $D_{298}$ ,  $E_d$  and  $D_0$  were calculated from a least-square fit of the data to Equation (3).  $D_{298}$  corresponds to room-temperature silver tracer diffusion coefficient  $D_{\text{Ag}}$ . The results are listed in Table 1 and shown in Figure 3.

The  $^{110m}\text{Ag}$  tracer diffusion coefficient decreases monotonically by 2.3 orders of magnitude with increasing  $x$  from  $6.8 \times 10^{-11} \text{ cm}^2 \text{ s}^{-1}$  ( $x = 0$ ) to  $3.8 \times 10^{-13} \text{ cm}^2 \text{ s}^{-1}$  ( $x = 0.15$ ) at room temperature (Table 1). Fig. 3a shows that the conductivity and tracer diffusion isotherms for the ternary CdTe-AgI-As<sub>2</sub>Te<sub>3</sub> glasses are significantly different, especially at  $x \geq 0.05$ . These results are consistent with our previous assumption<sup>19</sup> that the ternary glasses, depending on  $x$ , are either mixed or predominantly electronic conductors. Fig. 3b shows that the diffusion activation energy  $E_d$  increases simultaneously from 0.47 eV to 0.68 eV. Meanwhile, the pre-exponential factor  $D_0$  increases by a factor of 15 with increasing  $x$ , Fig. 3c. Similar increase of  $D_0$  was also observed in the  $(\text{CdSe})_x(\text{AgI})_{0.5-x/2}(\text{As}_2\text{Se}_3)_{0.5-x/2}$  system.<sup>19</sup> The diffusion pre-exponential factor is proportional to the attempt frequency  $v_0$ , the jump distance  $\ell$ , and the activation entropy for the jump of a mobile ion  $\Delta S^\#$

$$D_0 \propto v_0 \ell^2 \exp(\Delta S^\# / k), \quad (4)$$

where  $k$  is the Boltzmann constant. Neglecting the entropy term, the  $D_0$  increase may be related either to higher  $v_0$ , or to longer  $\ell$ . Taking into account the proposed immobilization of some Ag<sup>+</sup> cations by cadmium species within the preferential conduction pathways in the CdSe-AgI-As<sub>2</sub>Se<sub>3</sub> glasses<sup>19</sup>, the effective jump distance is expected to increase with  $x$ , thus increasing  $D_0$ .

### 3.2 Apparent Haven Ratio

The Haven ratio  $H_R$  is a simple experimental parameter easily accessible from a combined (tracer diffusion coefficient  $D$  and ionic conductivity  $\sigma_i$ ) experiment or from a single electro-diffusion or Chemla measurement. Since the total conductivity  $\sigma_{dc}$ , measured using impedance spectroscopy, is not purely ionic, i.e., the silver ion transport number  $t_{Ag^+} < 1$ , we cannot calculate the Haven ratio  $H_R^{20}$

$$H_R = \frac{D_{Ag}}{D_\sigma}, \quad (5)$$

where  $D_\sigma$  is the conductivity diffusion coefficient calculated from the ionic conductivity  $\sigma_i$  using the Nernst-Einstein relation

$$D_\sigma = \frac{kT\sigma_i}{N(ze)^2}, \quad (6)$$

where  $N$  is the concentration of the mobile species,  $ze$  is the electric charge of the carrier ion, and  $k$  and  $T$  have their usual meaning. However, we have calculated the apparent Haven ratio  $t_{Ag^+}H_R$  using the usual definition of the ion transport number

$$\sigma_i = t_{Ag^+} \sigma_{dc} \quad (7)$$

By combining the equations 5, 6 and 7, the apparent Haven ratio  $t_{Ag^+}H_R$  can be expressed as:

$$t_{Ag^+}H_R = \frac{D_{Ag}N(ze)^2}{kT\sigma} \quad (8)$$

The calculated  $t_{Ag^+}H_R$  are presented in Figure 4 as a function of temperature and their average values are also given in Table 1. The apparent Haven ratio decreases significantly with  $x$  from  $t_{Ag^+}H_R = 0.16 \pm 0.02$  for the  $x = 0$  glassy host,  $(AgI)_{0.5}(As_2Te_3)_{0.5}$ , to  $t_{Ag^+}H_R = (3.7 \pm 0.8) \times 10^{-4}$  for the  $x = 0.15$  glass at the limit of the glass-forming range. Since the overall changes of the Haven ratio in glasses and crystals are limited,  $0.2 \leq H_R \leq 1$  (see for example, references<sup>1,2,8,17,20</sup> and references therein), doping with CdTe results in a remarkable decrease of  $t_{Ag^+}$ , at least by two or three orders of magnitude, discussed in details in the next section.

### 3.3 Ionic versus Electronic Transport

Analysis of the total conductivity  $\sigma_{dc}$  and  $^{110m}Ag$  tracer diffusion  $D_{Ag}$  allows the ionic and electronic transport to be distinguished. Figure 5a shows the room-temperature conductivity  $\sigma_{dc}$  and its ionic counterpart  $H_R\sigma_{Ag^+}$ , calculated from  $D_{Ag}$  using Equations (5)

1  
2  
3 and (6). The two activation energies and pre-exponential factors are compared in Fig.  
4 5b and Fig. 5c.  
5

6 A non-monotonic change in  $\sigma_{dc}$  accompanied by a shallow maximum in the conductivity  
7 activation energy  $E_\sigma$  seems to be related to a crossover from the mixed conducting  
8 glasses with a significant contribution of the  $\text{Ag}^+$  ion transport to the CdTe-rich vitreous  
9 alloys having predominantly electronic conductivity. Similar phenomenon was  
10 observed in the binary  $(\text{AgI})_z(\text{As}_2\text{Te}_3)_{1-z}$  glassy system with variable silver iodide content  
11  $z$ .<sup>16,17</sup> The AgI-poor glasses are essentially electronic conductors but the  $\text{Ag}^+$  ion  
12 transport becomes predominant at  $z \geq 0.4$ . The most concentrated  $(\text{AgI})_{0.6}(\text{As}_2\text{Te}_3)_{0.4}$   
13 and  $(\text{AgI})_{0.8}(\text{As}_2\text{Te}_3)_{0.2}$  glasses appear to be nearly pure ionic conductors with  $t_{\text{Ag}^+} \cong 1$   
14 and  $t_{\text{Ag}^+} \gg t_e$ , where  $t_e = t_n + t_p$  is the electron transport number of  $n$ - and/or  $p$ -type.<sup>17</sup>  
15 Using the apparent Haven ratio  $t_{\text{Ag}^+}H_R$  for the ternary glasses, we can estimate the silver  
16 ion transport numbers  $t_{\text{Ag}^+}$  in this system. The Haven ratio for the ion-conducting glass  
17  $(\text{AgI})_{0.6}(\text{As}_2\text{Te}_3)_{0.4}$ ,  $H_R = 0.44 \pm 0.08$ , is very similar to those for AgI-rich superionic  
18  $(\text{AgI})_z(\text{As}_2\text{Se}_3)_{1-z}$  vitreous alloys,  $H_R = 0.40 \pm 0.04$  at  $z \geq 0.4$ .<sup>17,19</sup> Assuming that the  
19  $(\text{AgI})_{0.5}(\text{As}_2\text{Te}_3)_{0.5}$  glass also has  $H_R = 0.44$ , the calculated  $t_{\text{Ag}^+}$  values vary between 0.8  
20 and 0.2 for this particular composition, Figure 6.

21 The observed decrease of  $t_{\text{Ag}^+}$  with increasing temperature is expected since the  
22 diffusion activation energy  $E_d$  is lower than  $E_\sigma$ , Fig. 5b. In other words, the electronic  
23 conductivity increases faster with increasing temperature than the ionic transport,  
24 resulting in a  $t_{\text{Ag}^+}$  decrease,  $\partial t_{\text{Ag}^+} / \partial T < 0$ . In addition, we have observed earlier that the  
25 mixed conducting silver selenide and silver telluride glasses are characterized by higher  
26 values of the activation energy and pre-exponential factor related to electronic or hole  
27 transport.<sup>19,21,22</sup> In ion-conducting  $(\text{CdSe})_x(\text{AgI})_{0.5-x/2}(\text{As}_2\text{Se}_3)_{0.5-x/2}$  glasses, the Haven  
28 ratio increases with  $x$  from  $H_R = 0.4$  to 0.7.<sup>19</sup> Assuming similar trend for the ternary  
29 telluride system, we have calculated the silver ion transport numbers. The room  
30 temperature  $t_{\text{Ag}^+}$  values, shown in Figure 7, decrease exponentially with  $x$  from  
31  $0.67 \pm 0.15$  ( $x = 0$ ) to  $(6.6 \pm 1.8) \times 10^{-4}$  ( $x = 0.15$ ), i.e., by 3 orders of magnitude. The  
32 calculated  $t_{\text{Ag}^+}$  was used to divide the total conductivity  $\sigma_{dc}$  into ionic  $\sigma_{\text{Ag}^+}$  and electronic  
33  $\sigma_e$  parts, Figure 8.

34 The binary  $x = 0$  glassy host,  $(\text{AgI})_{0.5}(\text{As}_2\text{Te}_3)_{0.5}$ , is a mixed conductor with a significant  
35 contribution of the  $\text{Ag}^+$  ion conductivity,  $t_{\text{Ag}^+} = 0.67 \pm 0.15$ . Semiconducting CdTe  
36 additions induce two opposite processes: (1) a remarkable exponential decrease of the  
37 ion transport by a factor of  $\approx 200$ ; and (2) a monotonic increase of the electronic  
38 conductivity by  $\approx 1.5$  orders of magnitude. The crossover between the two regimes is  
39 reflected by a non-monotonic change in  $\sigma_{dc}$ . The electronic conductivity increase with  $x$   
40 is caused by Te 5p lone-pair electronic states in the top of the valence band.<sup>23</sup>

51  
52  
53  
54  
55  
56 **3.4 Suppression of the Ion Transport**  
57  
58  
59  
60

We have already reported similar decrease of the ionic conductivity  $\sigma_i$  and  $^{110m}\text{Ag}$  tracer diffusion  $D_{\text{Ag}}$  with increasing  $x$  in the ternary selenide system  $(\text{CdSe})_x(\text{AgI})_{0.5-x/2}(\text{As}_2\text{Se}_3)_{0.5-x/2}$ .<sup>18,19</sup> Comparing the ion transport parameters with those for the binary superionic  $\text{AgI}-\text{As}_2\text{Se}_3$  glasses, it was found that the ternary glasses with the same silver concentration exhibit much lower  $\sigma_i$  and  $D_{\text{Ag}}$ . A comparable effect is observed for the binary  $\text{AgI}-\text{As}_2\text{Te}_3$  and ternary  $\text{CdTe}-\text{AgI}-\text{As}_2\text{Te}_3$  glasses, Figure 9. The diffusion coefficient at 25 °C,  $D_{298}$ , for the ternary  $\text{CdTe}$ -rich glass ( $x = 0.15$ ) appears to be lower by  $\approx 2$  orders of magnitude in comparison with its binary counterpart, Fig. 9a. The respective diffusion activation energy is higher by 0.2 eV, Fig. 9b.

The remarkable suppression of the  $\text{Ag}^+$  ion transport with increasing  $\text{CdTe}$  content can also have chemical and structural origin similar to that in the selenide system.<sup>18,19</sup> The exchange reaction  $\text{CdTe} + 2\text{AgI} \rightleftharpoons \text{CdI}_2 + \text{Ag}_2\text{Te}$  in the glass-forming melt may lead to a mixed silver environment. As a result, the  $\text{Ag}^+$  ion mobility within the mixed iodide/telluride conduction pathways decreases. Nevertheless, the quantitative analysis of the chemical effect does not reproduce the observed ion transport changes in the ternary selenide glasses.<sup>18</sup> At  $x < 0.2$ , a significant difference still exists between the simulated and experimental conductivity. A non-random mixing of cadmium and silver species in the ternary glass network appears to be the basis of an additional and/or alternative structural interpretation. Cd-related structural units do not form separate domains but are positioning within the preferential conduction pathways built-up by Ag-related polyhedra. Immobile or slow  $\text{Cd}^{2+}$  ions will affect the  $\text{Ag}^+$  ion dynamics by restricting the number of accessible empty sites thus reducing the ionic conductivity. The observed increase of the Haven ratio in the selenide system with increasing  $x$  is consistent with the non-random mixing but implies immobilisation of some neighboring  $\text{Ag}^+$  cations by a  $\text{Cd}^{2+}$  ion.<sup>19</sup> Both chemical and structural reasons of the  $\text{Ag}^+$  ion transport suppression need further experimental verification in the ternary telluride system. The experimental conductivity and diffusion data alone do not allow any reliable evidence in favor of either hypothesis to be provided. High-energy x-ray diffraction results could provide a clue for solving the problem.

### 3.5 Transport Properties in the Telluride and Selenide Ternary Systems

The two ternary  $(\text{CdX})_x(\text{AgI})_{0.5-x/2}(\text{As}_2\text{X}_3)_{0.5-x/2}$  systems, where X = Se or Te, exhibit many similarities and characteristic differences in transport properties, Figure 10. First, the telluride glasses, as the vast majority of vitreous tellurides<sup>23,24</sup>, have a significantly higher electronic conductivity compared to their selenide counterparts,  $\approx 2$  orders of magnitude at 25 °C, Fig. 10a. The observed difference is caused by Te 5p lone-pair electron states forming the top of the valence band in telluride alloys compared to lower lying Se 4p lone pairs.<sup>23,25</sup>

On the contrary, the ionic conductivity and silver tracer diffusion coefficient are by a factor of 100 to 300 higher in the selenide ternaries, Fig. 10b, accompanied also by lower activation energy. Similar decrease of  $D_{\text{Ag}}$  was reported earlier for mixed chalcogen Ag-As-Se-Te glasses<sup>21</sup>, when Se was progressively replaced by Te. Only the intermediate compositions with Te fraction  $r = \text{Te}/(\text{Se}+\text{Te})$  in the range of  $0.05 \leq r \leq 0.35$ , have shown a non-monotonic change in  $D_{\text{Ag}}$ , attributed to a mixed anion effect. The reason of the observed difference in the magnitude of  $\sigma_i$  and  $D_{\text{Ag}}$  between telluride and selenide systems is not yet clear. Detailed structural studies are needed to compare the connectivity of Ag-related sub-network in the two families. Finally, the effect of CdX (X = Se or Te) additions is identical for the two systems. Semiconducting cadmium chalcogenides increase the electronic conductivity and decrease the ionic one. Even quantitatively, the observed changes are similar:  $D_{\text{Ag}}$  decreases of 2-2.5 orders of magnitude and  $\sigma_e$  increases by a factor of 10-30.

#### 4. CONCLUSIONS

The  $^{110}\text{mAg}$  tracer diffusion coefficient in the  $(\text{CdTe})_x(\text{AgI})_{0.5-x/2}(\text{As}_2\text{Te}_3)_{0.5-x/2}$  glasses ( $0.0 \leq x \leq 0.15$ ) decreases by a factor of  $\approx 200$  with increasing  $x$  from  $6.8 \times 10^{-11} \text{ cm}^2 \text{ s}^{-1}$  ( $x = 0.0$ ) to  $3.8 \times 10^{-13} \text{ cm}^2 \text{ s}^{-1}$  ( $x = 0.15$ ) at room temperature. The  $D_{\text{Ag}}$  decrease is accompanied by a simultaneous increase of the diffusion activation energy from 0.47 eV to 0.68 eV and the diffusion pre-exponential factor by a factor of 15. The combined analysis of diffusion and conductivity data shows a significant decrease of the silver ion transport number by three orders of magnitude with increasing  $x$ . The suppression of the  $\text{Ag}^+$  ion transport accompanied by a simultaneous increase of the electronic conductivity causes an ionic-to-electronic transport crossover in cadmium telluride glasses; the CdTe-rich vitreous alloys become nearly pure electronic conductors.

#### AUTHOR INFORMATION

##### Corresponding Author

\*E-mail: Mohamad.Kassem@univ-littoral.fr. Phone: +33-328-658270.

##### Author Contributions

The manuscript was written through contributions of all authors. All authors have given approval to the final version of the manuscript.

##### Notes

The authors declare no competing financial interest.

#### ACKNOWLEDGMENTS

This work was supported by the European Commission within the Interreg IIIA (CTMM project) and Interreg IVA (CleanTech project) programmes and by Agence Nationale de la Recherche (ANR, France) under Grant No. ANR-15-ASTR-0016-01.

**RERERENCES**

- (1) Terai, R.; Hayami, R. Ionic Diffusion in Glasses. *J. Non-Cryst. Solids* **1975**, *18*, 217–264.
- (2) Frischat, G.H. Ionic Diffusion in Oxide Glasses. *Trans Tech Publications* **1975**.
- (3) Natrup, F.V.; Bracht, H.; Murugavel, S.; Roling, B. Cation Diffusion and Ionic Conductivity in Soda-Lime Silicate Glasses. *Phys. Chem. Chem. Phys.* **2005**, *7*, 2279–2286.
- (4) Mehrer, H.; Imre, A. W.; Tanguep-Nijocep, E. Diffusion and Ionic Conduction in Oxide Glasses. *J. Phys. Conf. Series* **2008**, *106*, 012001
- (5) Kawamoto, Y.; Nishida, M. Silver Diffusion in As<sub>2</sub>S<sub>3</sub>-Ag<sub>2</sub>S, GeS<sub>2</sub>-GeS-Ag<sub>2</sub>S and P<sub>2</sub>S<sub>5</sub>-Ag<sub>2</sub>S Glasses. *Phys. Chem. Glasses* **1977**, *18*, 19–23.
- (6) Kazakova, E.A. A Study of Silver-Containing Chalcogenide Glasses. Leningrad University: Ph.D. Thesis. Leningrad, **1980**.
- (7) Thomas, M.P.; Peterson, N.L.; Hutchinson, E. Tracer Diffusion and Electrical Conductivity in Sodium-Rubidium Silicon Sulfide Glasses. *J. Am. Ceram. Soc.* **1985**, *68*, 99–104.
- (8) Bychkov, E.; Tsegelnik, V.; Vlasov, Yu.; Pradel, A.; Ribes, M. Percolation Transition in Ag-Doped Germanium Chalcogenide-Based Glasses: Conductivity and Silver Diffusion Results. *J. Non-Cryst. Solids* **1996**, *208*, 1–20.
- (9) Bychkov, E.; Bychkov, A.; Pradel, A.; Ribes, M. Percolation Transition in Ag-Doped Chalcogenide Glasses: Comparison of Classical Percolation and Dynamic Structure Models. *Solid State Ionics* **1998**, *113–115*, 691–695.
- (10) Drugov, Yu.; Tsegelnik, V.; Bolotov, A.; Vlasov, Yu.; Bychkov, E. <sup>110</sup>Ag Tracer Diffusion Study of Percolation Transition in Ag<sub>2</sub>S-As<sub>2</sub>S<sub>3</sub> Glasses. *Solid State Ionics* **2000**, *136–137*, 1091–1096.
- (11) Bychkov, E.; Bolotov, A.; Tsegelnik, V.; Grushko, Yu.; Vlasov, Yu. <sup>64</sup>Cu Tracer Diffusion in Copper Chalcogenide Glasses. *Defect Diffus. Forum* **2001**, *194–199*, 919–924.
- (12) Bychkov, E.; Bolotov, A.; Grushko, Y.S.; Vlasov, Yu.; Wortmann, G. Ionic Diffusion and Local Hopping in Copper Chalcohalide Glasses Measured Using <sup>64</sup>Cu Tracer and <sup>129</sup>I-Mössbauer Spectroscopy. *Solid State Ionics* **1996**, *90*, 289–294.
- (13) Bychkov, E.; Bolotov, A.; Armand, P.; Ibanez, A. EXAFS Studies of Cu<sup>+</sup> Ion Conducting and Semiconducting Copper Chalcogenide and Chalcohalide Glasses. *J. Non-Cryst. Solids* **1998**, *232–234*, 314–322.

- (14) Bolotov, A.; Bychkov, E.; Gavrilov, Yu.; Grushko, Yu.; Pradel, A.; Ribes, M.; Tsegelnik, V.; Vlasov, Yu. Degenerated Mixed Cation Effect in CuI-AgI-As<sub>2</sub>Se<sub>3</sub> Glasses: <sup>64</sup>Cu and <sup>110</sup>Ag Tracer Diffusion Studies. *Solid State Ionics* **1998**, *113–115*, 697–701.
- (15) Kassem, M.; Le Coq, D.; Boidin, R.; Bychkov, E. New Chalcogenide Glasses in the CdTe-AgI-As<sub>2</sub>Te<sub>3</sub> System. *Materials Research Bulletin* **2012**, *47*, 193–198.
- (16) Bobylev, Yu.V.; Bychkov, E.A.; Tver'yanovich, Yu.S. Electrical Properties of Glasses in the AgI-As<sub>2</sub>Te<sub>3</sub> System. *Glass Physics and Chemistry* **2004**, *30*, 519–522.
- (17) Alekseev, I.; Kassem, M.; Fourmentin, M.; Le Coq, D.; Iizawa, R.; Usuki, T.; Bychkov, E. Ionic and Electronic Transport in AgI-As<sub>2</sub>Te<sub>3</sub> Glasses. *Solid State Ionics* **2013**, *253*, 181–184.
- (18) Kassem, M.; Le Coq, D.; Bokova, M.; Bychkov, E. Chemical and Structural Origin of Conductivity Changes in CdSe-AgI-As<sub>2</sub>Se<sub>3</sub> Glasses. *Solid State Ionics* **2010**, *181*, 466–472.
- (19) Alekseev, I.; Kassem, M.; Le Coq, D.; Bokova, M.; Fourmentin, M.; Bychkov, E. <sup>110</sup>Ag Tracer Diffusion Studies of CdSe-AgI-As<sub>2</sub>Se<sub>3</sub> Glasses. *Solid State Ionics* **2010**, *181*, 1467–1472.
- (20) Murch, G.E. The Haven Ratio in Fast Ionic Conductors. *Solid State Ionics* **1982**, *7*, 177–198.
- (21) Vlasov, Yu.G.; Bychkov, E.A.; Seleznev, B.L. Compositional Dependence of Ionic Conductivity and Diffusion in Mixed Chalcogen Ag-Containing Glasses. *Solid State Ionics* **1987**, *24*, 179–187.
- (22) Vlasov, Yu.G.; Bychkov, E.A. Ionic and Electronic Conductivity in the Copper-Silver-Arsenic-Selenium Glasses. *Solid State Ionics* **1984**, *14*, 329–335.
- (23) Mott, N.F.; Davis, E.A. Electronic Processes in Non-Crystalline Materials. Clarendon Press, Oxford, **1979**.
- (24) Adam J.-L.; Zhang, X. (Editors) Chalcogenide Glasses: Preparation, properties and applications. Woodhead Publishing, Oxford – Cambridge – Philadelphia – New Delhi, **2014**.
- (25) Kolobov, A. V.; Tominaga, J. Chalcogenides. Metastability and Phase Change Phenomena. Springer, Heidelberg – New York – Dordrecht – London, **2012**.

## List of Figures

- 1  
2  
3  
4  
5  
6  
7  
8  
9  
10  
11  
12  
13  
14  
15  
16  
17  
18  
19  
20  
21  
22  
23  
24  
25  
26  
27  
28  
29  
30  
31  
32  
33  
34  
35  
36  
37  
38  
39  
40  
41  
42  
43  
44  
45  
46  
47  
48  
49  
50  
51  
52  
53  
54  
55  
56  
57  
58  
59  
60  
1. Typical  $^{110m}\text{Ag}$  tracer diffusion profile for a  $(\text{CdTe})_{0.05}(\text{AgI})_{0.475}(\text{As}_2\text{Te}_3)_{0.475}$  glass annealed at 45 °C for 17 days. The filled circles correspond to penetration depth calculated using weight changes; the open symbols represent direct thickness measurements. The solid line shows a least-square fit of the experimental data points to Equation (2) where  $q = \text{erf}^{-1}\left(1 - \frac{A(y, t)}{A_0}\right)$ .
2. Temperature dependences of the silver tracer diffusion coefficient for glasses in the ternary system  $(\text{CdTe})_x(\text{AgI})_{0.5-x/2}(\text{As}_2\text{Te}_3)_{0.5-x/2}$ . The solid lines represent a least-square fit of the data to Equation (3).
3. Composition dependences of both (●) diffusion and (●) conductivity parameters for the ternary  $(\text{CdTe})_x(\text{AgI})_{0.5-x/2}(\text{As}_2\text{Te}_3)_{0.5-x/2}$  glasses: (a) room-temperature silver tracer diffusion coefficient  $D_{\text{Ag}}$  and conductivity diffusion coefficient  $D_{\sigma}$  calculated using the Nernst-Einstein relation; (b) diffusion activation energy  $E_d$ ; (c) diffusion pre-exponential factor  $D_0$ . All solid lines are drawn as a guide to the eye.
4. Apparent Haven ratio  $t_{\text{Ag}^+}H_R$  for the CdTe-AgI-As<sub>2</sub>Te<sub>3</sub> glasses plotted as a function of temperature.
5. Total conductivity  $\sigma_{dc}$  and ionic transport parameters for the ternary CdTe-AgI-As<sub>2</sub>Te<sub>3</sub> glasses: (a) room-temperature  $\sigma_{dc}$  and  $H_R\sigma_{\text{Ag}^+}$ ; (b) the conductivity  $E_{\sigma}$  and diffusion  $E_d$  activation energies, and (c) the conductivity  $\sigma_0$  and recalculated diffusion  $H_R\sigma_0(\text{Ag}^+)$  pre-exponential factors. All solid lines are a guide to the eye.
6. Silver ion transport number  $t_{\text{Ag}^+}$  plotted as a function of temperature for selected  $(\text{CdTe})_x(\text{AgI})_{0.5-x/2}(\text{As}_2\text{Te}_3)_{0.5-x/2}$  glasses,  $x = 0$  and 0.05.
7. Room temperature silver ion transport number  $t_{\text{Ag}^+}$  for the ternary  $(\text{CdTe})_x(\text{AgI})_{0.5-x/2}(\text{As}_2\text{Te}_3)_{0.5-x/2}$  glasses plotted as a function of CdTe content.

- 1  
2  
3     8. Room temperature total conductivity  $\sigma_{dc}$  as well as its ionic  $\sigma_{Ag^+}$  and electronic  $\sigma_e$   
4       components for the ternary CdTe-AgI-As<sub>2</sub>Te<sub>3</sub> glasses.  
5  
6  
7     9. (a) Room temperature diffusion coefficient  $D_{Ag}$ , and (b) diffusion activation  
8       energy  $E_d$  for the binary AgI-As<sub>2</sub>Te<sub>3</sub><sup>17</sup> and ternary CdTe-AgI-As<sub>2</sub>Te<sub>3</sub> glasses  
9       plotted as a function of the silver content. The solid lines are drawn as a guide to  
10      the eye.  
11  
12  
13  
14  
15     10. Room-temperature transport characteristics of the ternary (CdX)<sub>x</sub>(AgI)<sub>0.5-x/2</sub>  
16       (As<sub>2</sub>X<sub>3</sub>)<sub>0.5-x/2</sub> glasses, where X = Se or Te: (a) electronic conductivity; (b) <sup>110m</sup>Ag  
17       tracer diffusion coefficient.  
18  
19  
20  
21  
22  
23  
24  
25  
26  
27  
28  
29  
30  
31  
32  
33  
34  
35  
36  
37  
38  
39  
40  
41  
42  
43  
44  
45  
46  
47  
48  
49  
50  
51  
52  
53  
54  
55  
56  
57  
58  
59  
60

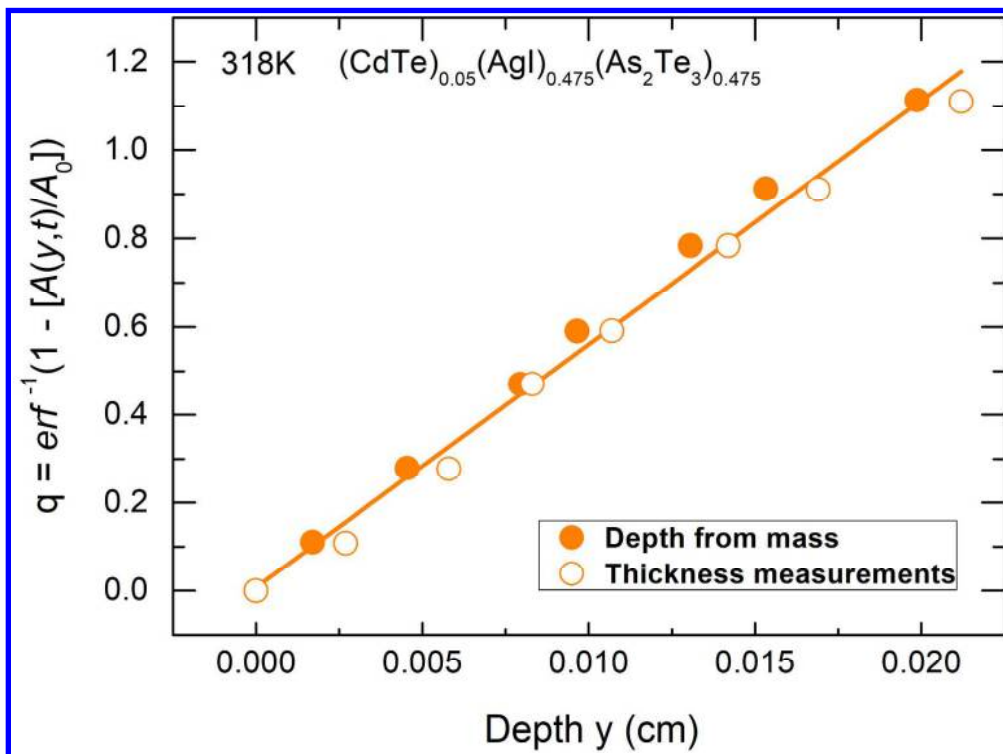


**Fig. 1.** Typical <sup>110</sup>mAg tracer diffusion profile for a (CdTe)<sub>0.05</sub>(AgI)<sub>0.475</sub>(As<sub>2</sub>Te<sub>3</sub>)<sub>0.475</sub> glass annealed at 45 °C for 17 days. The penetration depth was calculated using (a) weight changes (filled circles) and (b) direct thickness measurements (open circles). The solid line shows a least-square fit of all experimental data points (open and filled circles) to Equation (2) where  $q = \text{erf}^{-1}\left(1 - \frac{A(y,t)}{A_0}\right)$ .

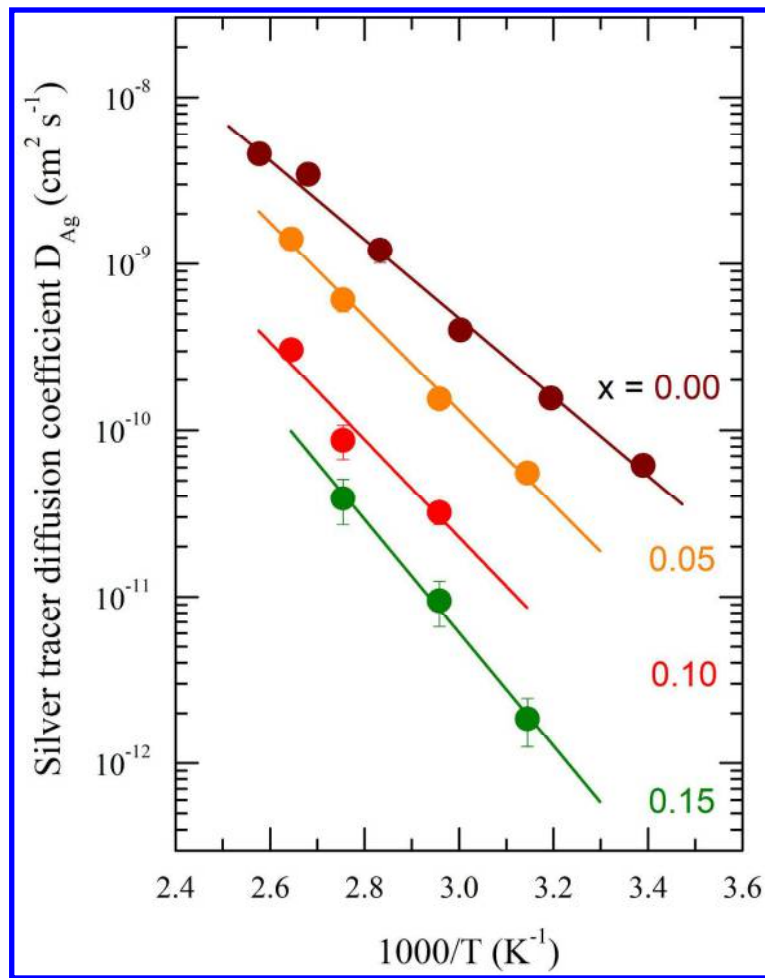


**Fig. 2.** Temperature dependences of the silver tracer diffusion coefficient for glasses in the ternary system  $(\text{CdTe})_x(\text{AgI})_{0.5-x/2}(\text{As}_2\text{Te}_3)_{0.5-x/2}$ . The solid lines represent a least-square fit of the data to Equation (3).

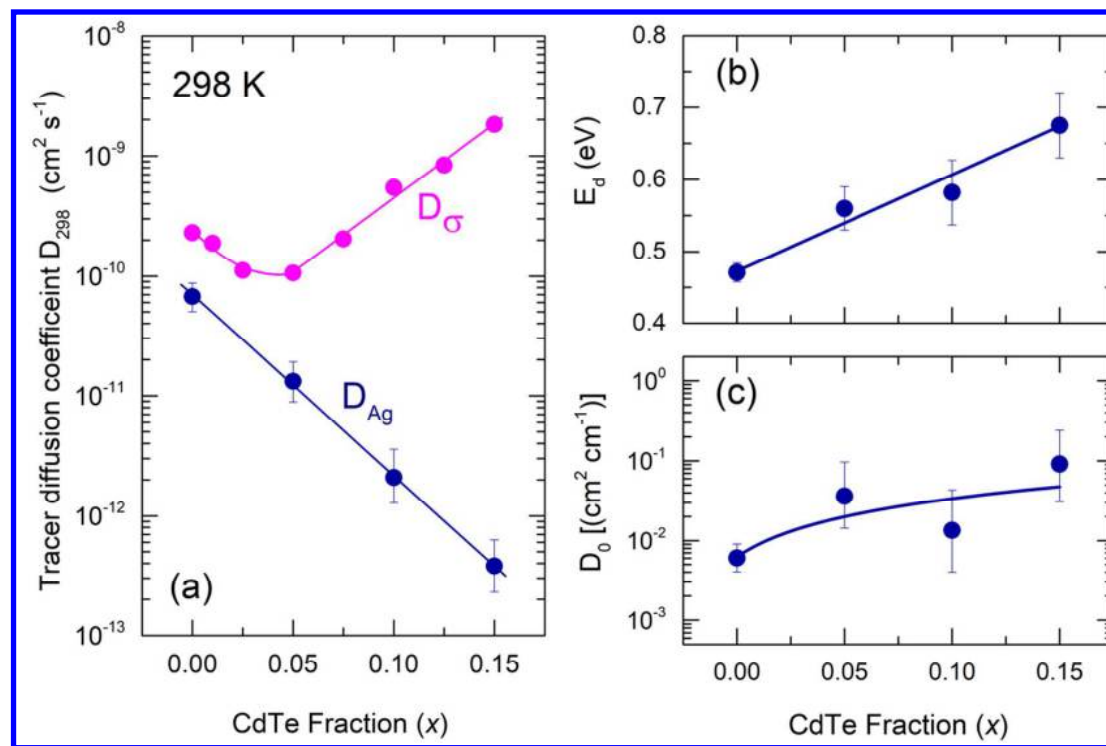


**Fig. 3.** Composition dependences of both (●) diffusion and (○) conductivity parameters for the ternary  $(\text{CdTe})_x(\text{AgI})_{0.5-x/2}(\text{As}_2\text{Te}_3)_{0.5-x/2}$  glasses: (a) room-temperature silver tracer diffusion coefficient  $D_{\text{Ag}}$  and conductivity diffusion coefficient calculated using the Nernst-Einstein relation; (b) diffusion activation energy  $E_d$ ; (c) diffusion pre-exponential factor  $D_0$ . All solid lines are drawn as a guide to the eye.

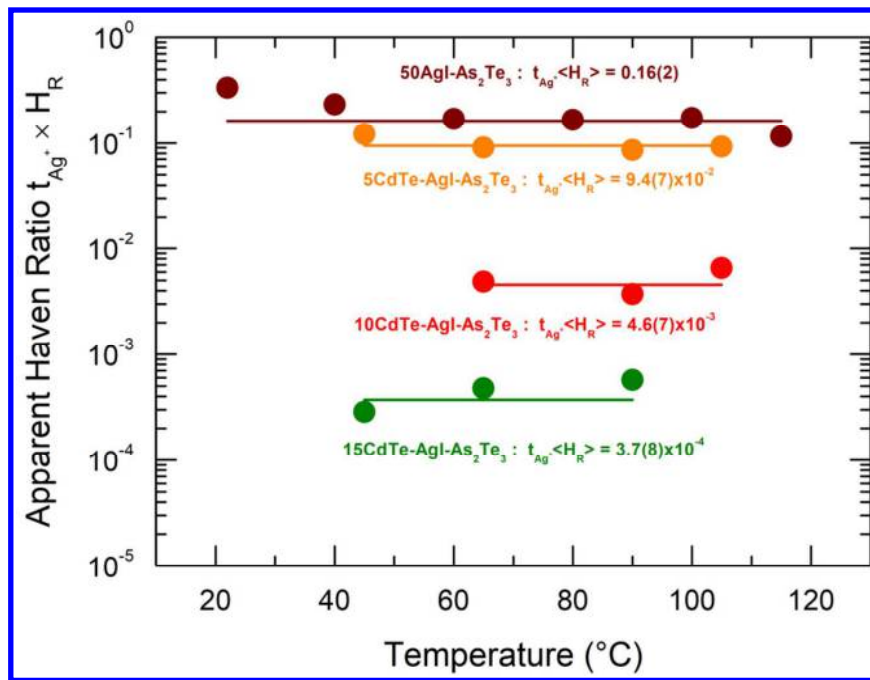


**Fig. 4.** Apparent Haven ratio  $t_{Ag^+}H_R$  for the CdTe-AgI-As<sub>2</sub>Te<sub>3</sub> glasses plotted as a function of temperature.

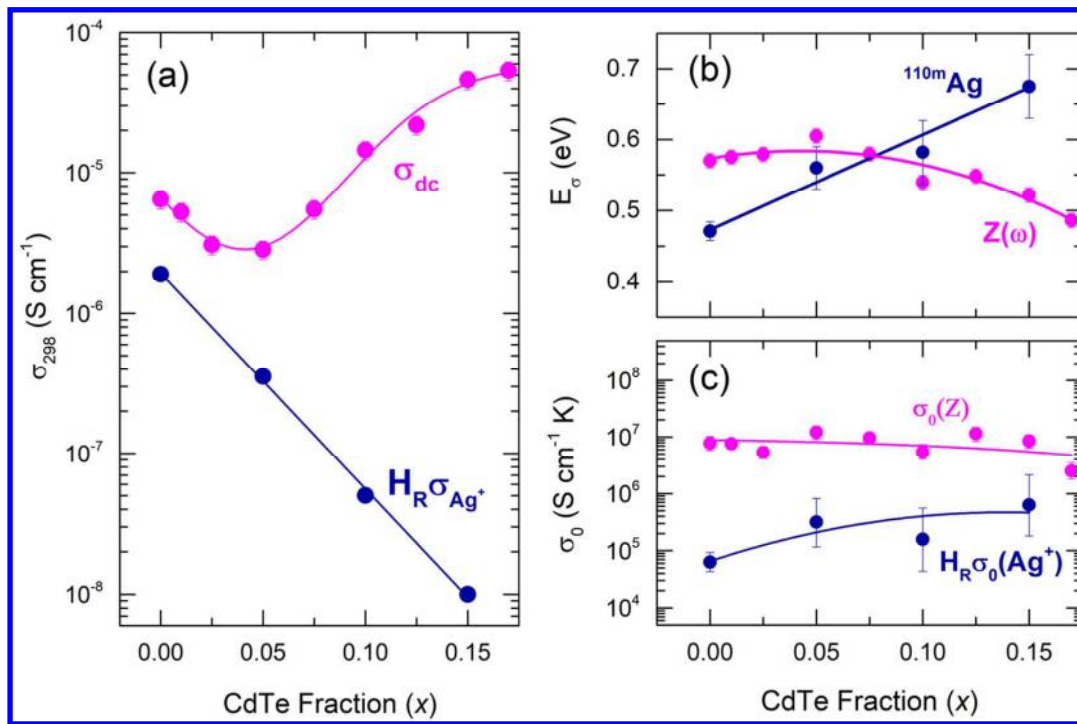


**Fig. 5.** Total conductivity  $\sigma_{dc}$  and ionic transport parameters for the ternary CdTe-AgI-As<sub>2</sub>Te<sub>3</sub> glasses: (a) room-temperature  $\sigma_{dc}$  and  $H_R\sigma_{Ag^+}$ ; (b) the conductivity  $E_\sigma$  and diffusion  $E_d$  activation energies, and (c) the conductivity  $\sigma_0$  and recalculated diffusion  $H_R\sigma_0(Ag^+)$  pre-exponential factors. All solid lines are a guide to the eye.

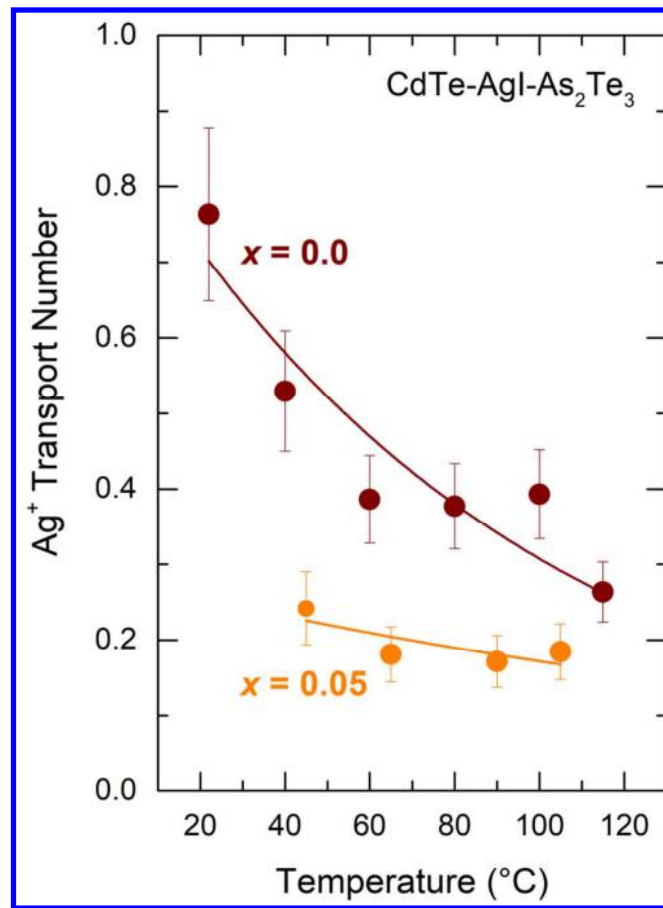


**Fig. 6.** Silver ion transport number  $t_{Ag^+}$  plotted as a function of temperature for selected  $(CdTe)_x(AgI)_{0.5-x/2}(As_2Te_3)_{0.5-x/2}$  glasses,  $x = 0$  and  $0.05$ .

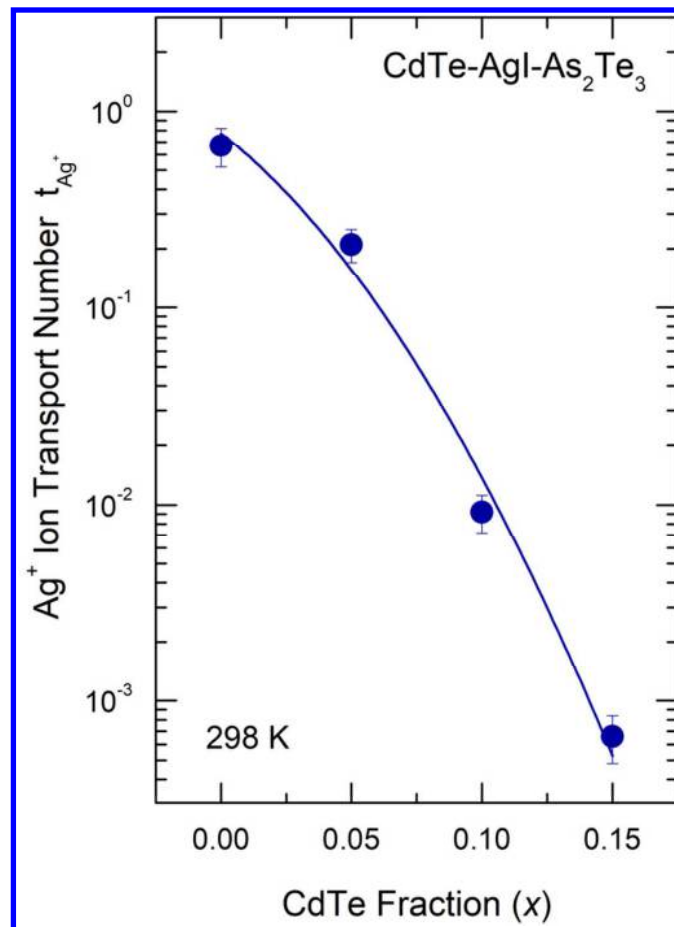


**Fig. 7.** Room temperature silver ion transport number  $t_{\text{Ag}^+}$  for the ternary  $(\text{CdTe})_x(\text{AgI})_{0.5-x/2}(\text{As}_2\text{Te}_3)_{0.5-x/2}$  glasses plotted as a function of CdTe content.

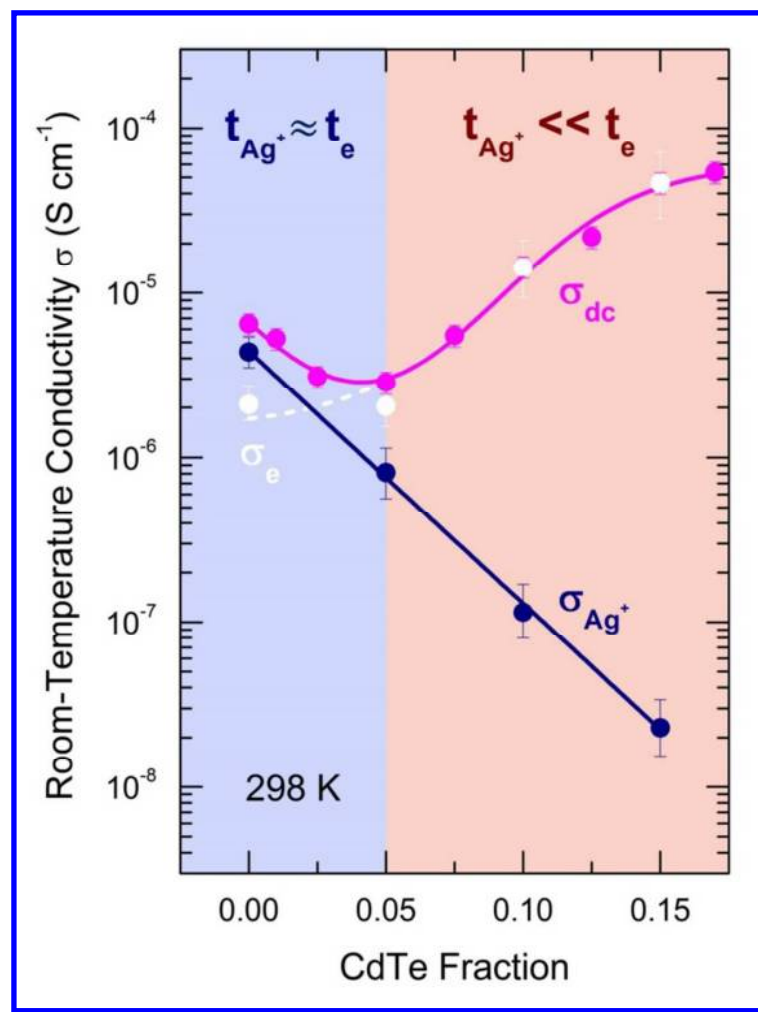


**Fig. 8.** Room temperature total conductivity  $\sigma_{dc}$  as well as its ionic  $\sigma_{\text{Ag}^+}$  and electronic  $\sigma_e$  components for the ternary CdTe-AgI-As<sub>2</sub>Te<sub>3</sub> glasses.

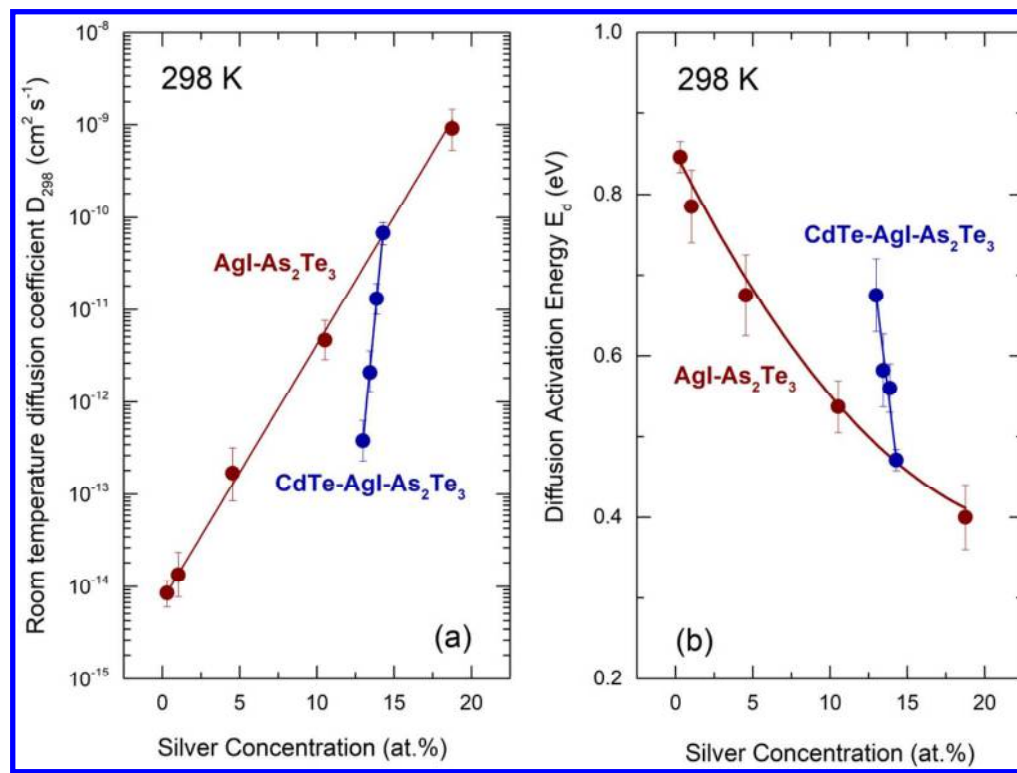
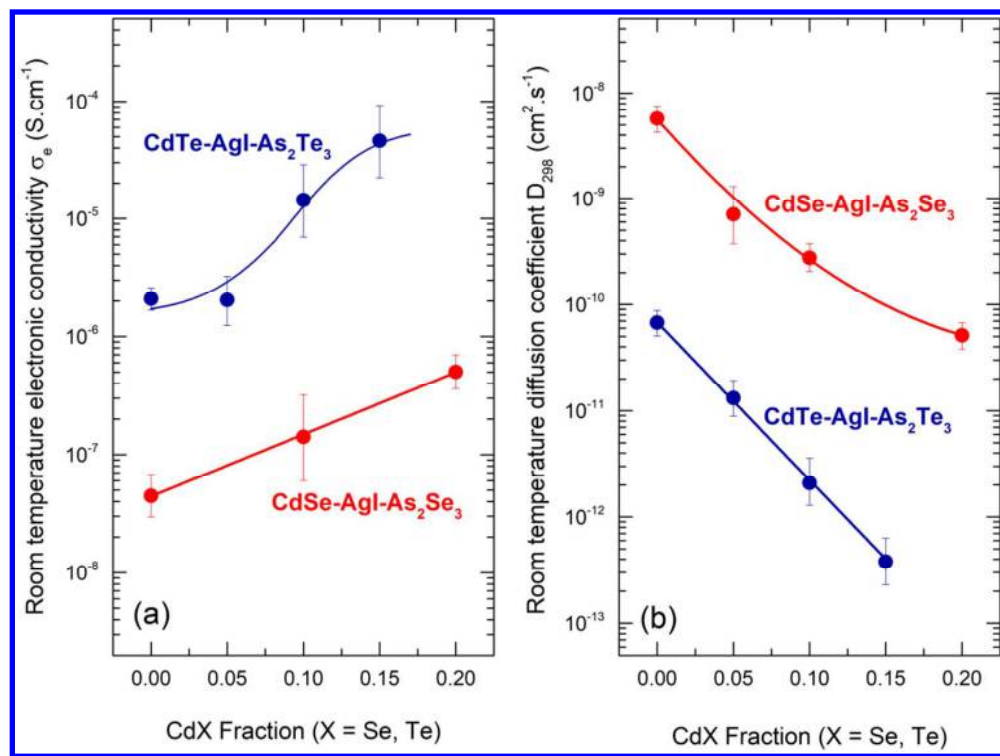


**Fig. 9.** (a) Room temperature diffusion coefficient  $D_{\text{Ag}}$ , and (b) diffusion activation energy  $E_a$  for the binary  $\text{AgI-As}_2\text{Te}_3^{17}$  and ternary  $\text{CdTe-AgI-As}_2\text{Te}_3$  glasses plotted as a function of the silver content. The solid lines are drawn as a guide to the eye.



1  
2  
3 **List of Tables**  
4  
5  
6

7     1.  $^{110m}\text{Ag}$  tracer diffusion parameters for the CdTe-AgI-As<sub>2</sub>Te<sub>3</sub> glasses: the room-  
8     diffusion coefficient  $D_{298}$ , the diffusion activation energy  $E_d$ , the pre-exponential  
9     factor  $D_0$ , and the apparent Haven ratio  $t_{\text{Ag}^+}H_R$   
10  
11  
12  
13  
14

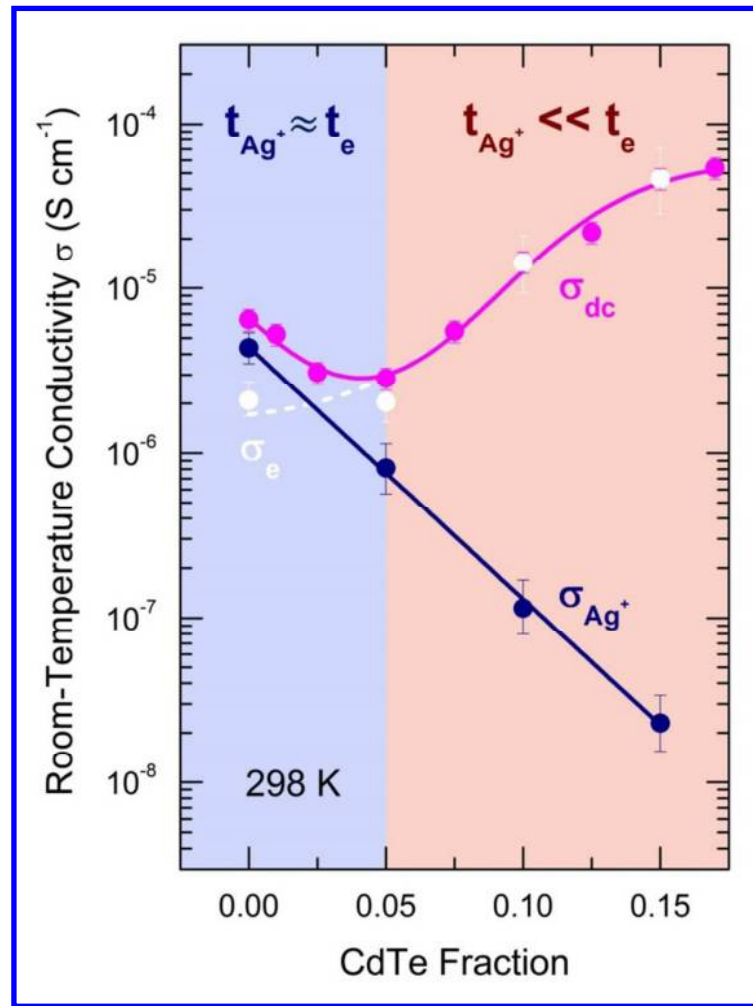
15 **Table 1**  
16

17      $^{110m}\text{Ag}$  tracer diffusion parameters for the CdTe-AgI-As<sub>2</sub>Te<sub>3</sub> glasses: the room-diffusion  
18     coefficient  $D_{298}$ , the diffusion activation energy  $E_d$ , the pre-exponential factor  $D_0$ , and the  
19     apparent Haven ratio  $t_{\text{Ag}^+}H_R$

<i>Composition</i>	$D_{298}$ (cm <sup>2</sup> s <sup>-1</sup> )	$E_d$ (eV)	$D_0$ (cm <sup>2</sup> s <sup>-1</sup> )	$t_{\text{Ag}^+}H_R$
$(\text{CdTe})_x(\text{AgI})_{0.5-x/2}(\text{As}_2\text{Te}_3)_{0.5-x/2}$				
<i>x</i>	[Ag] (at.%)			
0.00	14.28	$6.8 \times 10^{-11}$	0.471(13)	$6.0 \times 10^{-3}$
0.05	13.87	$1.3 \times 10^{-11}$	0.560(31)	$3.6 \times 10^{-2}$
0.10	13.43	$2.1 \times 10^{-12}$	0.582(45)	$1.3 \times 10^{-2}$
0.15	12.98	$3.8 \times 10^{-13}$	0.675(46)	$9.1 \times 10^{-2}$

20     Uncertainties in the last digit(s) of the parameter are given in parentheses.  
21  
22

23     The apparent Haven ratio  $t_{\text{Ag}^+}H_R$  averaged over the temperature range of diffusion measurements.  
24  
25  
26  
27  
28  
29  
30  
31  
32  
33  
34  
35  
36  
37  
38  
39  
40  
41  
42  
43  
44  
45  
46  
47  
48  
49  
50  
51  
52  
53  
54  
55  
56  
57  
58  
59  
60

TOC graphic

<i>Composition</i>	$D_{298}$ (cm <sup>2</sup> s <sup>-1</sup> )	$E_d$ (eV)	$D_0$ (cm <sup>2</sup> s <sup>-1</sup> )	$t_{Ag} H_R$
$(CdTe)_x(AgI)_{0.5-x/2}(As_2Te_3)_{0.5-x/2}$				
<i>x</i>	[Ag] (at.%)			
0.00	14.28	6.8×10 <sup>-11</sup>	0.471(13)	6.0×10 <sup>-3</sup>
0.05	13.87	1.3×10 <sup>-11</sup>	0.560(31)	3.6×10 <sup>-2</sup>
0.10	13.43	2.1×10 <sup>-12</sup>	0.582(45)	1.3×10 <sup>-2</sup>
0.15	12.98	3.8×10 <sup>-13</sup>	0.675(46)	9.1×10 <sup>-2</sup>

*Uncertainties in the last digit(s) of the parameter are given in parentheses.*  
*The apparent Haven ratio  $t_{Ag} H_R$  averaged over the temperature range of diffusion measurements.*

<sup>110m</sup>Ag tracer diffusion parameters for the CdTe-AgI-As<sub>2</sub>Te<sub>3</sub> glasses: the room-diffusion coefficient  $D_{298}$ , the diffusion activation energy  $E_d$ , the pre-exponential factor  $D_0$ , and the apparent Haven ratio  $t_{Ag} H_R$

248x84mm (96 x 96 DPI)

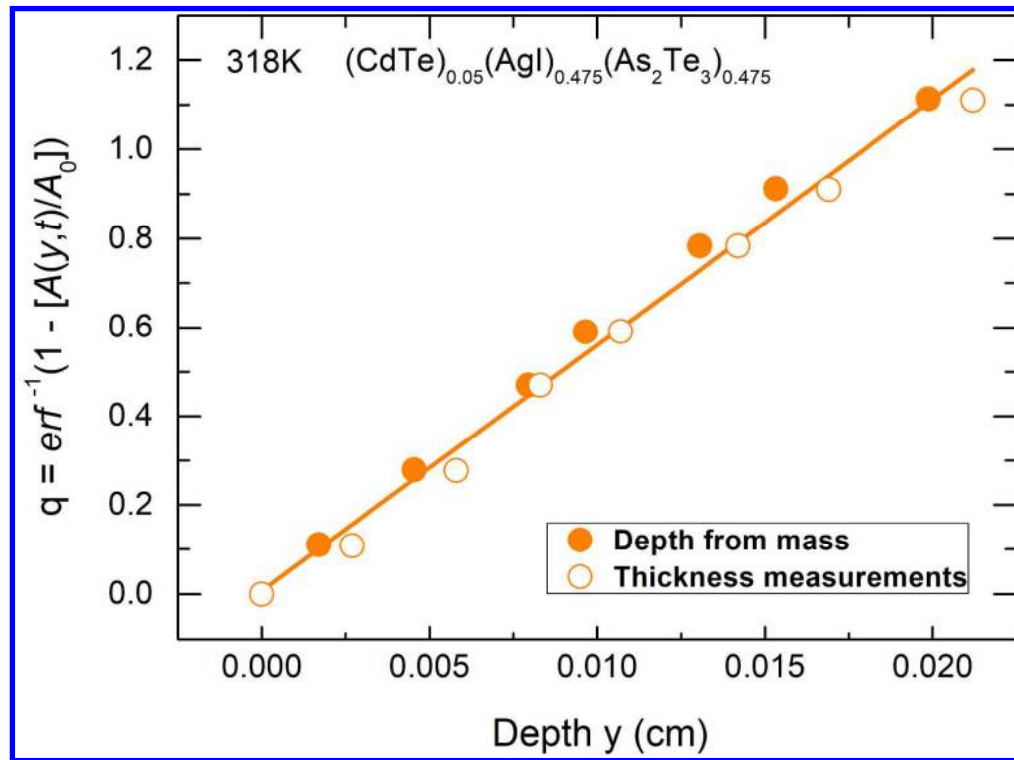


Figure 1. Typical  $^{110}\text{mAg}$  tracer diffusion profile for a  $(\text{CdTe})_{0.05}(\text{AgI})_{0.475}(\text{As}_2\text{Te}_3)_{0.475}$  glass annealed at 45 °C for 17 days. The penetration depth was calculated using (a) weight changes (filled circles) and (b) direct thickness measurements (open circles). The solid line shows a least-square fit of all experimental data points (open and filled circles) to Equation (2) where  $q = \text{erf}^{-1}(1 - A(y,t)/A_0)$ .

241x179mm (300 x 300 DPI)

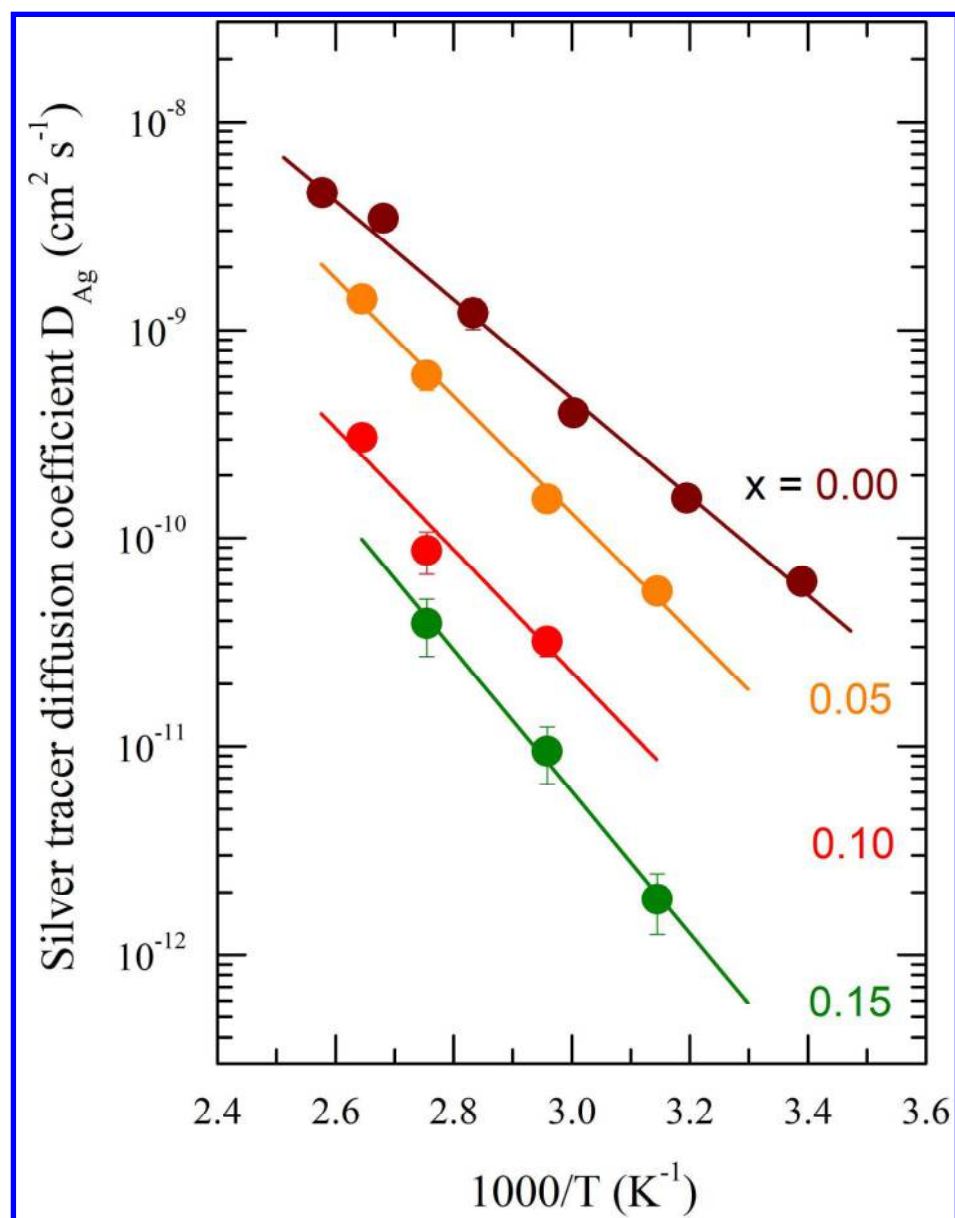


Figure 2. Temperature dependences of the silver tracer diffusion coefficient for glasses in the ternary system  $(\text{CdTe})_x(\text{AgI})_{0.5-x/2}(\text{As}_2\text{Te}_3)_{0.5-x/2}$ . The solid lines represent a least-square fit of the data to Equation (3).

182x234mm (300 x 300 DPI)

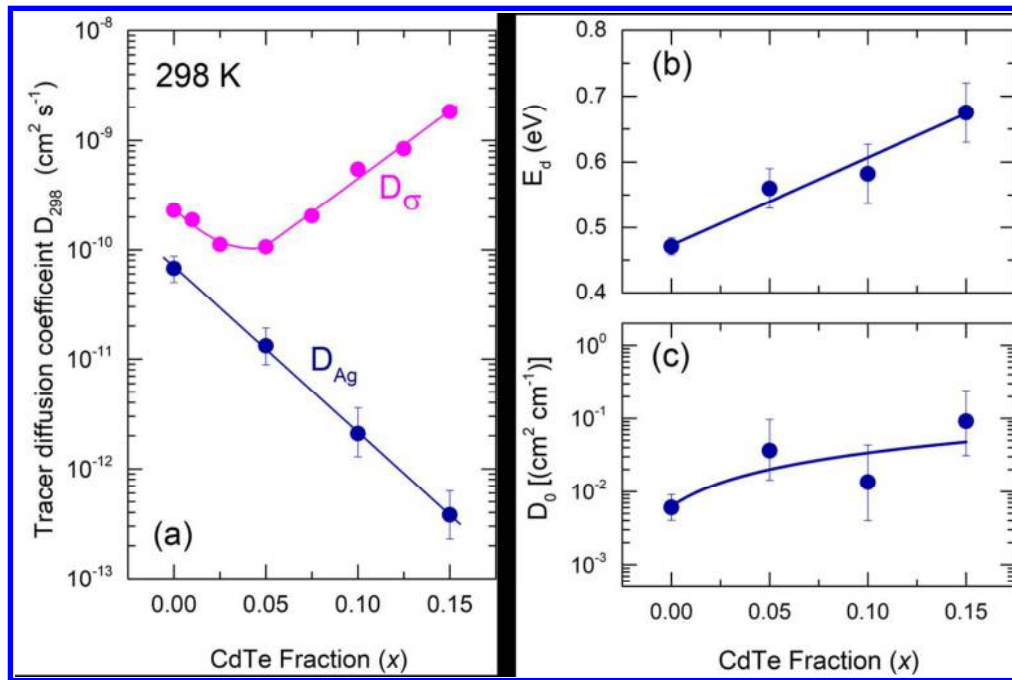


Figure 3. Composition dependences of both (●) diffusion and (●) conductivity parameters for the ternary  $(\text{CdTe})_x(\text{AgI})_{0.5-x/2}(\text{As}_2\text{Te}_3)_{0.5-x/2}$  glasses: (a) room-temperature silver tracer diffusion coefficient  $D_{\text{Ag}}$  and conductivity diffusion coefficient  $D_\sigma$  calculated using the Nernst-Einstein relation; (b) diffusion activation energy  $E_d$ ; (c) diffusion pre-exponential factor  $D_0$ . All solid lines are drawn as a guide to the eye.

233x154mm (150 x 150 DPI)

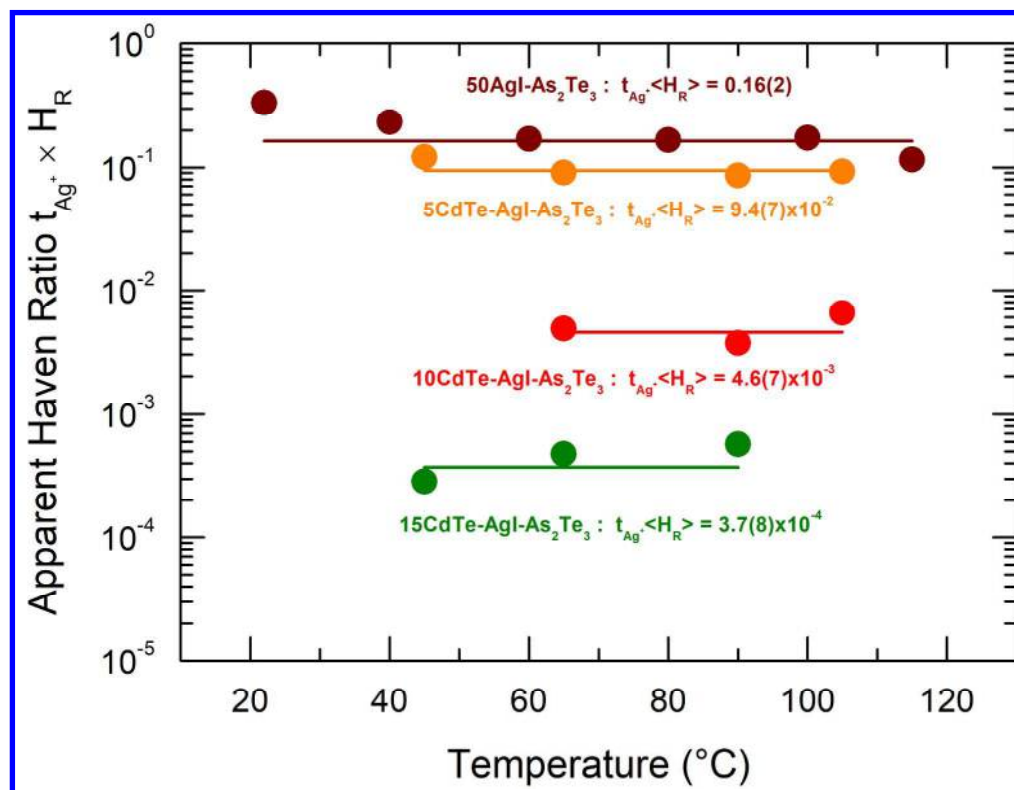


Figure 4. Apparent Haven ratio  $t_{Ag^+} H_R$  for the CdTe-AgI-As<sub>2</sub>Te<sub>3</sub> glasses plotted as a function of temperature.

234x180mm (300 x 300 DPI)

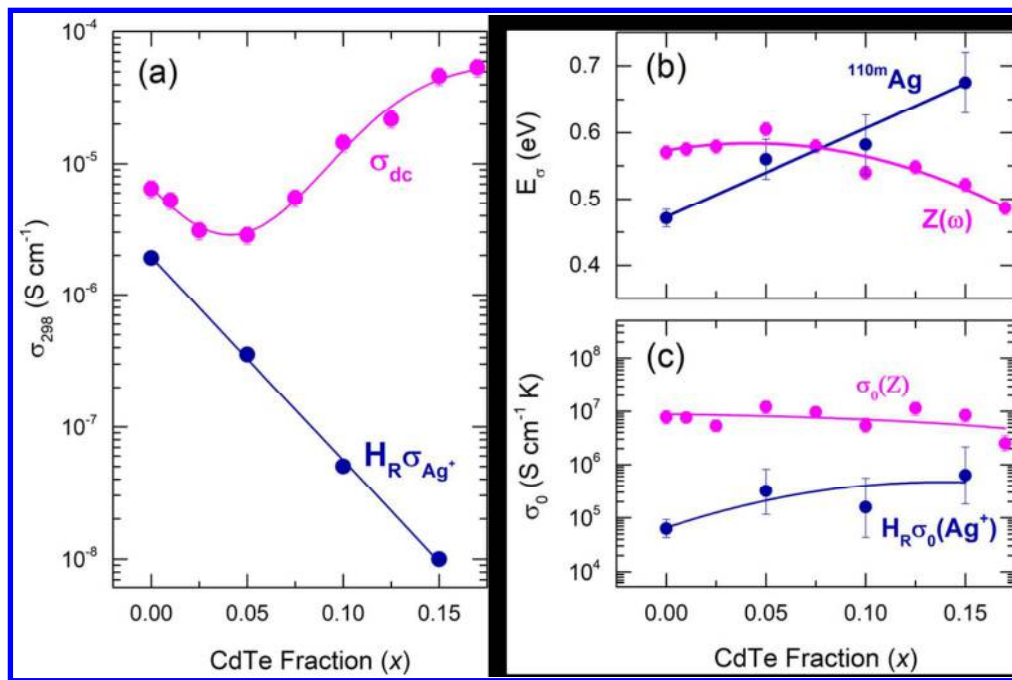


Figure 5. Total conductivity  $\sigma_{dc}$  and ionic transport parameters for the ternary CdTe-AgI-As<sub>2</sub>Te<sub>3</sub> glasses: (a) room-temperature  $\sigma_{dc}$  and  $H_R\sigma_{Ag^+}$ ; (b) the conductivity  $E_\sigma$  and diffusion  $E_d$  activation energies, and (c) the conductivity  $\sigma_0$  and recalculated diffusion  $H_R\sigma_0(Ag^+)$  pre-exponential factors. All solid lines are a guide to the eye.

230x152mm (150 x 150 DPI)

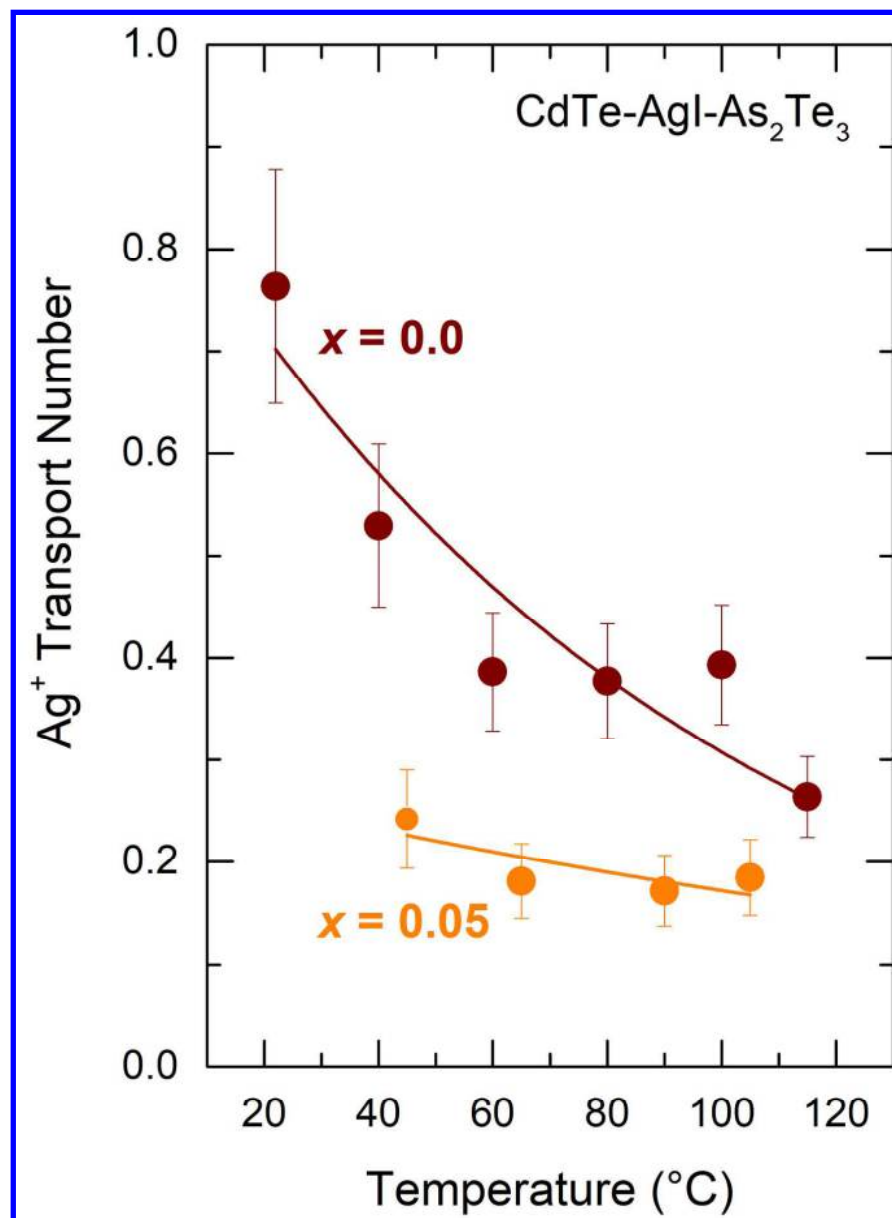


Figure 6. Silver ion transport number  $t_{Ag^+}$  plotted as a function of temperature for selected  $(CdTe)_x(AgI)_{0.5-x/2}(As_2Te_3)_{0.5-x/2}$  glasses,  $x = 0$  and  $0.05$ .

183x250mm (300 x 300 DPI)

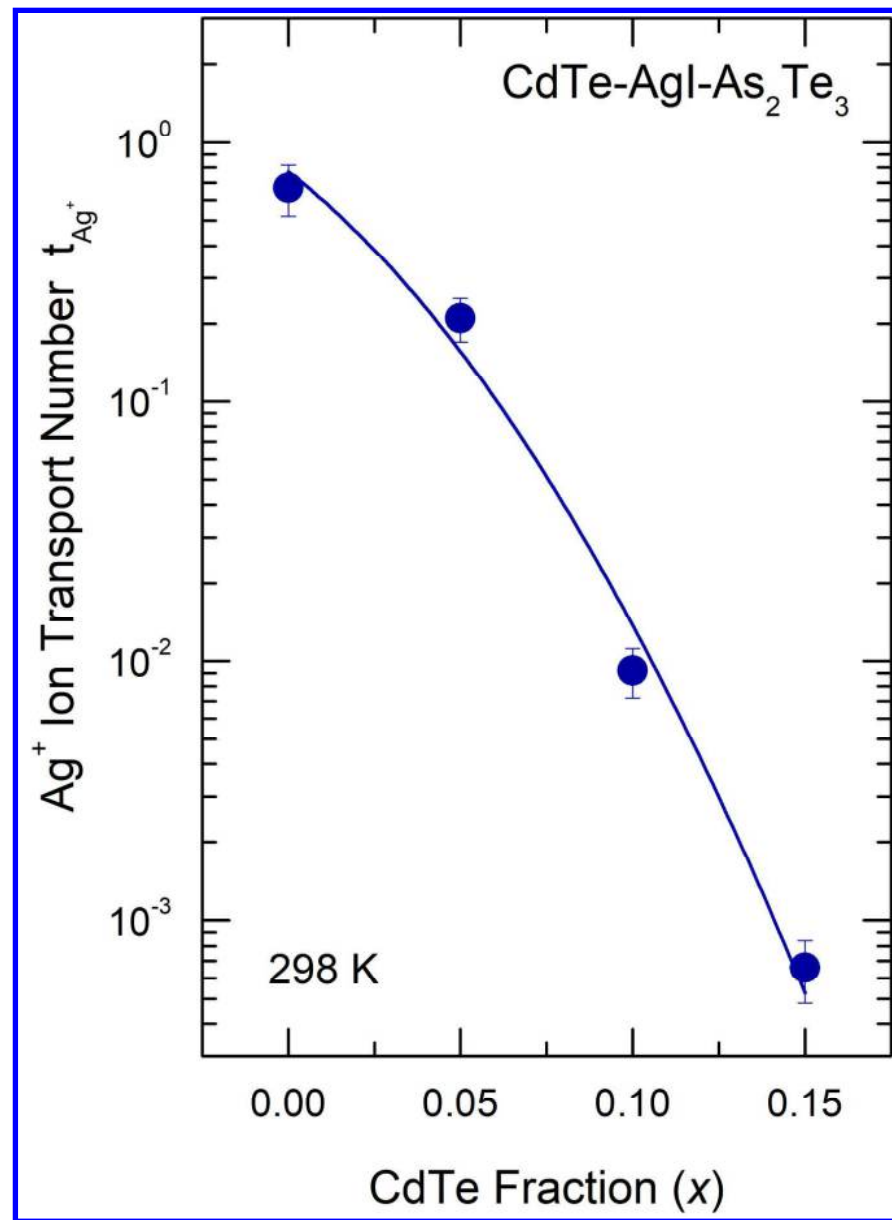


Figure 7. Room temperature silver ion transport number  $t_{Ag^+}$  for the ternary  $(CdTe)_x(AgI)_{0.5-x/2}(As_2Te_3)_{0.5-x/2}$  glasses plotted as a function of CdTe content.

174x239mm (300 x 300 DPI)

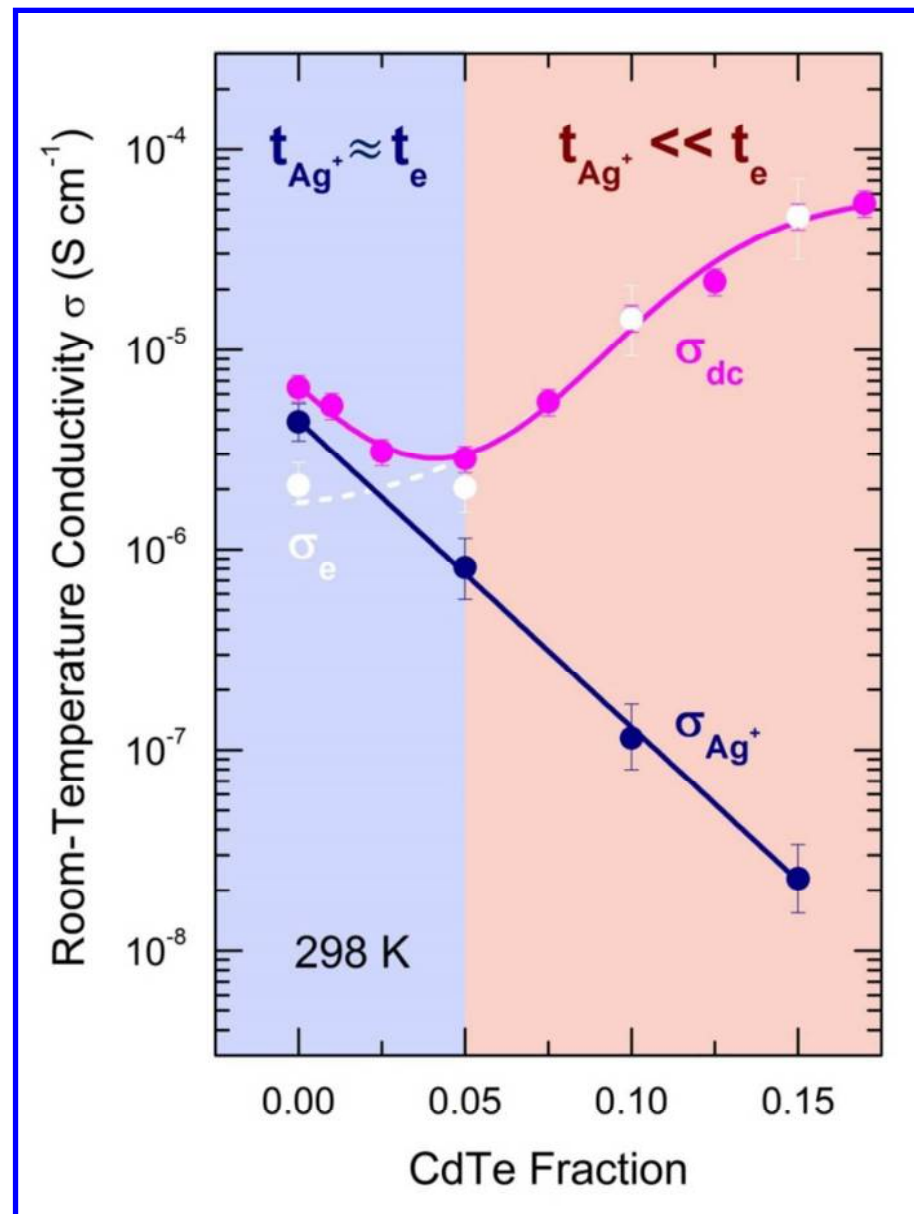


Figure 8. Room temperature total conductivity  $\sigma_{dc}$  as well as its ionic  $\sigma_{Ag^+}$  and electronic  $\sigma_e$  components for the ternary CdTe-AgI-As<sub>2</sub>Te<sub>3</sub> glasses.

97x129mm (220 x 220 DPI)

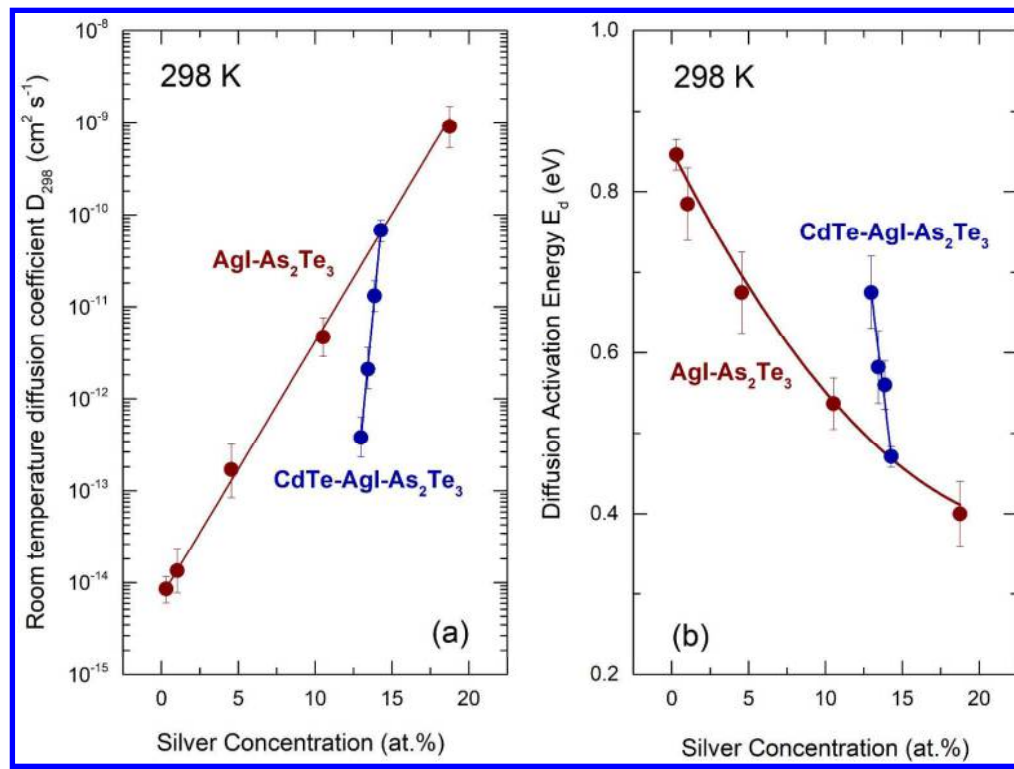


Figure 9. (a) Room temperature diffusion coefficient  $D_{\text{Ag}}$ , and (b) diffusion activation energy  $E_d$  for the binary  $\text{AgI-As}_2\text{Te}_3^{17}$  and ternary  $\text{CdTe-AgI-As}_2\text{Te}_3$  glasses plotted as a function of the silver content. The solid lines are drawn as a guide to the eye.

410x306mm (300 x 300 DPI)

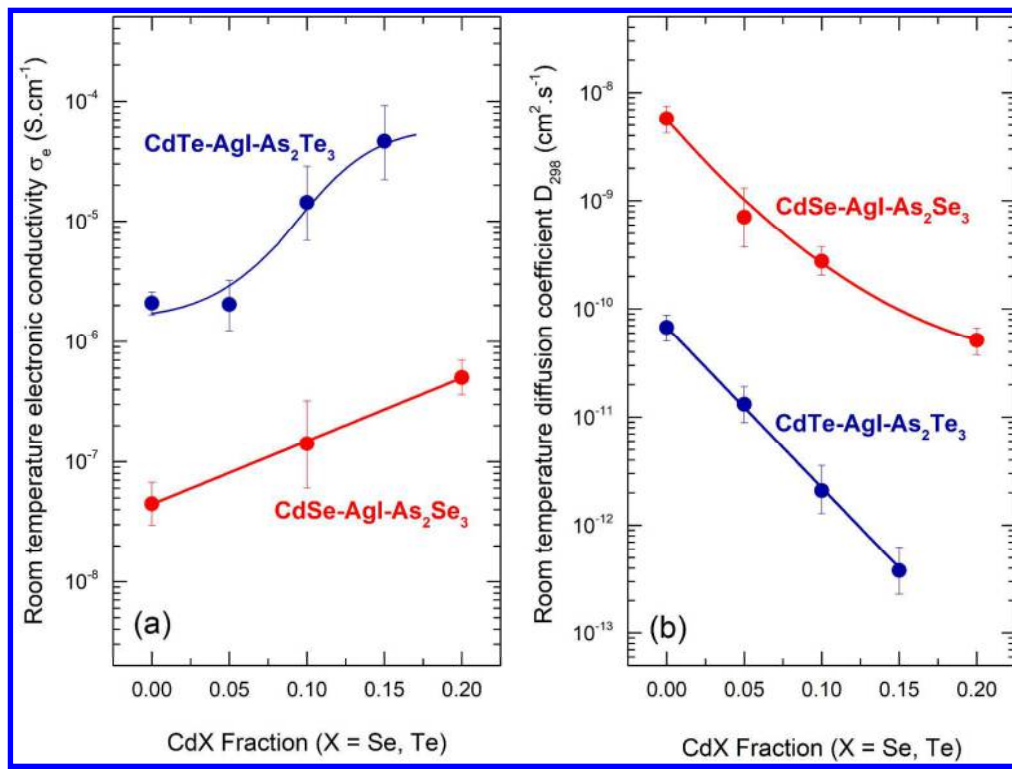


Figure 10. Room-temperature transport characteristics of the ternary  $(\text{CdX})_x(\text{AgI})_{0.5-x/2}(\text{As}_2\text{X}_3)_{0.5-x/2}$  glasses, where X = Se or Te: (a) electronic conductivity; (b)  $^{110m}\text{Ag}$  tracer diffusion coefficient.

407x304mm (300 x 300 DPI)